Available online at www.sciencedirect.com
ScienceDirect
Earth and Planetary Science Letters 267 (2008) 100–106
EPSL
www.elsevier.com/locate/epsl

Paleo-viscometry of magma bodies

Tobias Höink *, Cin-Ty A. Lee, Jessica C. Hawthorne, Adrian Lenardic

Department of Earth Science, Rice University, 6100 Main St, Houston, TX 77005, USA

Received 11 July 2007; received in revised form 1 October 2007; accepted 17 November 2007
Available online 8 December 2007
Editor: C.P. Jaupart

Abstract

Viscosity and water content are among the most important characteristics of magma bodies. However, once magma has erupted or solidified, such properties of the original magma are difficult to constrain directly. For an ensemble of rhythmically layered magmatic sills and dikes we present a simple model of crystallization and crystal settling that allows one to obtain a melt viscosity estimate when combined with field observations. If the composition of the parental magma is roughly known and an estimate of its liquidus temperature is known, the viscosity can be used to infer water content.

Keywords: paleo-viscometry; viscosity; water content; crystal nucleation; crystal settling; physical properties of magma

1. Introduction

Viscosity is one of the most fundamental properties of a magma because it controls, to first order, how a magma flows and erupts. Viscosity is also important because it is primarily influenced by temperature, major and minor element composition, and water content (Dingwell, 1995; Hui and Zhang, 2007). Water content itself plays an important role in the nature of magma genesis and global geochemical cycles (Kelley et al., 2006). However, the water content remains a rather elusive quantity. For example, it is difficult to determine pre-eruptive water contents of lavas because the effect of eruptive degassing on loss of water is difficult to determine. In addition, the measured water content of ancient magmas are often compromised by weathering, alteration, and metamorphism (Parman et al., 1997). Clearly, if the viscosity of a magma can be independently determined or measured, some of the above variables can be constrained. The problem is that there is no direct way to measure the viscosity of magmas, especially after they have cooled and solidified.

In an attempt to rectify this problem, we show here that under certain conditions, magma viscosity can potentially be inferred from measurable observations in the field at the outcrop level. Our investigation is based on rhythmic layering in cumulates found in layered sills and large flows. These rhythmic layers are composed of cyclic meter-scale sections of cumulates, which are themselves internally sorted on smaller lengthscales (centimeter) according to phenocryst grain size and density. Of interest here is the significance of these repetitive large-scale layers, not the small-scale internal layers.

Layering in magmatic bodies has been studied previously, in case studies (e.g. Pons et al., 2006), in laboratory settings (e.g. Martin and Nokes, 1988; Koyaguchi et al., 1990; Sparks et al., 1993) and numerical experiments (e.g. Rudman, 1992; Gibb and Henderson, 1992; Hort et al., 1993). Previous analytic studies of magma bodies include work by Zieg and Marsh (2002). In contrast to previous work, in which time-forward models required one to enter physical parameters a priori, we show how field observations linked with the physics of crystal settling in magma bodies establish an inverse problem which can be solved for pre-eruptive properties.

2. Motivating observations

Our analysis was motivated by an example of cumulate layering as discussed above within a gabbroic (basaltic andesite) sill in Big Bend National Park located in west Texas, United States of America (N 29° 4′ 37.1″, W 103° 6′ 22.1″).

* Corresponding author.
E-mail address: Tobias.Hoeink@rice.edu (T. Höink).

0012-821X/$ - see front matter © 2007 Elsevier B.V. All rights reserved.
doi:10.1016/j.epsl.2007.11.046

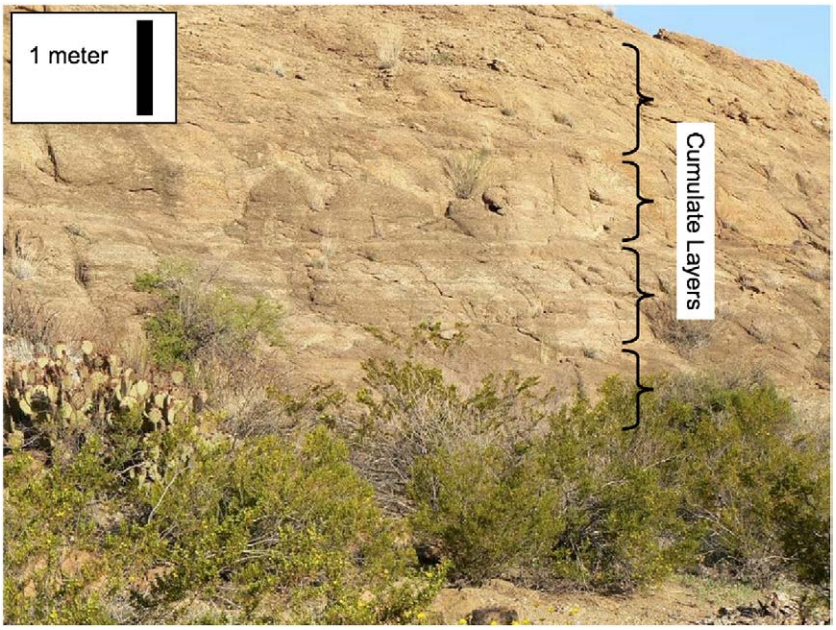

Fig. 1. Outcrop of layered sill in Big Bend National Park, Texas (USA). Brackets denote the meter-scale layers, each of which are presumably associated with a single flushing event of crystals formed in the sill. Fine-scale layering associated with internal segregation can also be seen.

The sill is associated with widespread late Tertiary volcanism throughout much of western North America and was emplaced into late Mesozoic carbonate sediments. It measures approximately 4 km by 2 km and is roughly 20 m thick. Most of the sill appears to be composed of layered cumulates, dominated by millimeter-sized crystals of plagioclase, hornblende, and magnetite (no quartz). The presence of hornblende indicates that the parental magma was hydrous, but this alone cannot constrain the actual weight percent of water in the parental magma. The layering in the sill is manifested on meter and centimeter lengthscales (Fig. 1). The centimeter-scale layering appears to be associated with density sorting of crystals during their accumulation. The meter-scale layering, which is the one of interest here, is characterized by 1–2 m thick crystallization sequences. These sequences can be seen on the outcrop scale by subtle changes in color and in degree of physical and chemical weathering. The latter is manifested by distinct topographic changes in the exposed outcrop. There is no field evidence to suggest that these layers were formed by in situ crystallization from the floor and ceiling walls inward as there is no hint of any symmetrical zonation in crystalline products. The characteristic time scale for conductive cooling of a 20 m (50 m) thick sill is about 3 yr (21 yr), which exceeds the estimated time scale for the settling of 2 mm crystals, 1.6 yr (2.2 yr). These observations suggest that layering in this sill originated by internal crystal nucleation followed by settling of these crystals. This interpretation, in turn, motivated a conceptual model for cumulate layering which we describe below.

3. Conceptual model

We begin with the following scenario for forming rhythmic large-scale layering in a magma chamber. We specifically confine our analysis to sills and dikes, which represent a class of magma bodies that are sufficiently large to retain heat for an extended period of time. Such a body cools by thermal diffusion on a time scale of $t_{\text{cooling}} = H^2/4\kappa$, where H is the characteristic length scale (thickness) of the sill and κ is the thermal diffusivity (Table 1). This time scale is on the order of years to tens of years for magma bodies of 10 to 100 m thickness. A number of studies have reached the conclusion that layering in km-scale magma bodies most likely occurs via in situ crystallization, wherein crystallization of the magma occurs in place from the chamber walls inward (Naslund and McBirney, 1996; Campbell, 1996). A detailed review is given by Marsh (2000). In a large magma chamber, the interior cools too slowly so that crystal nucleation within the magma chamber is suppressed. In an alternative scenario, the magma chamber interior cools at higher rates so as to allow homogeneous nucleation to occur in the interior, e.g. away from the chamber walls (Campbell, 1996). Crystals formed in the interior of a magma chamber are initially suspended by convective currents (see Fig. 2a for a schematic). Convection can be vigorous at this stage, based on an estimate of the Rayleigh number of 4×10^9 for a melt without crystals, assuming a viscosity of 1000 Pa s and a 20 m thick sill. As the crystal volume fraction increases due to continued nucleation and growth, the viscosity of the crystal–melt mixture increases strongly (Spera, 2000). For example, at a volume fraction of 20% the viscosity increases by two orders of magnitude (Tonks and Melosh, 1990), and the negative buoyancy of the crystals exceeds thermal density contrasts. These two effects, the strong viscosity increase (Solomatov and Stevenson, 1993) and negative buoyancy due to crystal mass (Koyaguchi et al., 1993), act in concert to suppress vigorous convection. Crystals formed in the interior of a magma chamber can then sink owing to their negative buoyancies (Fig. 2b), and the time

Table 1
Notation list

Quantity	Meaning	Unit
g	Acceleration due to gravity	m s^{-2}
G	Crystal growth rate	m s^{-1}
h	Height of crystal layer	m
J	Nucleation rate	$m^{-3}s^{-1}$
H	Height of the magmatic body	m
N	Number density of crystals	# m^{-3}
R	Crystal radius	m
R_{cr}	Critical crystal radius	m
t	Time	s
$t_{solidify}$	Time scale for solidification	s
t_{flush}	Time scale for "flushing"	s
t_{St}	Time scale of crystal settling	s
v_{St}	Stokes' velocity	m s^{-1}
η	Melt viscosity	Pa s
η_{crit}	Critical melt viscosity	Pa s
$\Delta\rho$	Crystal/melt density difference	kg m^{-3}
Φ	Volume fraction of crystals	%
$\Phi_{solidify}$	Critical volume fraction of crystals	%

scale of crystal settling is given by the Stokes' velocity of the largest crystals. For example, a crystal with 1 mm radius and a density contrast of 500 kg m^3 with respect to the melt will sink across a 20 m column of melt in about 2 yr, when the melt has a of viscosity of 1000 Pa s. The accumulation or sedimentation of these crystals to the bottom of the magma chamber generates layering (Fig. 2c), which is what concerns us here.

Qualitatively, the thicknesses of these layers should correlate with viscosity as follows. Because the sinking velocity of a crystal scales with the square of its radius, its settling velocity progressively increases as it grows. At some critical radius, the settling velocity is fast enough that the crystals quickly settle out of the magma chamber. When the largest crystals sink, viscous and buoyancy forces act on the smaller crystals, and the entire crystal population flushes to the bottom of the magma chamber. The time it takes for the largest crystals to settle out of the magma chamber is the flush time. Within this time scale all crystals are flushed out of the interior of the magma chamber and go on to form a thick layer of cumulates at the base of the magma chamber (Sparks et al., 1993). Each flushing event is followed by renewed crystal nucleation and growth, setting the stage for the deposition of another layer of cumulates (Fig. 2c). Our intuition leads us to suggest that high nucleation rates and growth rates yield a greater mass of accumulated crystals per unit time while higher viscosity should increase the flush time, allowing for a larger integrated mass of cumulates. Thus, if the crystal growth and nucleation rates are known within reasonable bounds, the characteristic thickness of cumulate layers should correlate with viscosity, in effect, giving us a field-based paleo-viscometer.

4. Mathematical model

We now explore these concepts more quantitatively. We begin with the approximation that the rate of crystal nucleation J is constant. Therefore, the number density of crystals N (number of crystals per unit volume) increases linearly with time t.

$$N(t) = Jt \tag{1}$$

Once crystals have nucleated they begin to grow. Existing growth rate laws have different grain size dependencies according to the underlying growth mechanism (Burton et al., 1951; Nielsen, 1964; Ohara and Reid, 1973). The most common growth mechanism for minerals is independent of the crystal size (Sunagawa, 1984). We therefore assume a constant growth rate G, i.e. the crystal radius R increases linearly with time.

$$R(t) = Gt. \tag{2}$$

The volume fraction of crystals inside the magma body will increase as the number density of crystals and their size

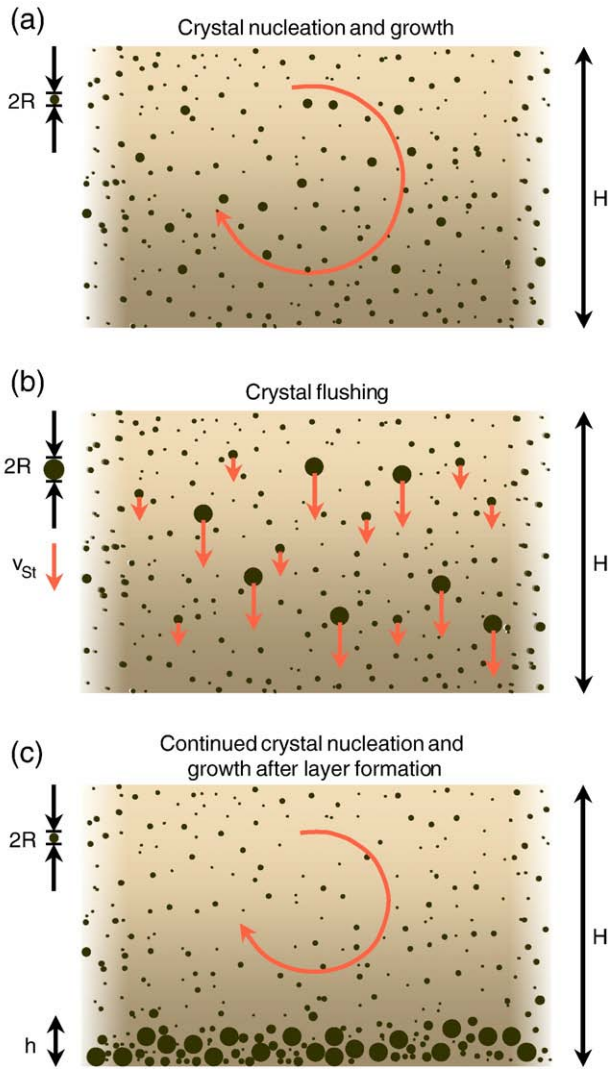

Fig. 2. Schematic illustrating the conceptual model. Repetitive layers are assumed to be formed in several stages. a: Cooling allows crystal nucleation and growth in the interior of the magma body. At this stage crystals are kept suspended by vigorous thermal convection. b: Thermally driven convection is stalled by increased viscosity and negative buoyancy due to a higher crystal fraction. Crystals sink to the bottom of the magma chamber. The largest crystals sink fastest and set the time scale. c: After crystals have sedimented, a new cycle begins with crystal nucleation and growth in the remaining magma chamber.

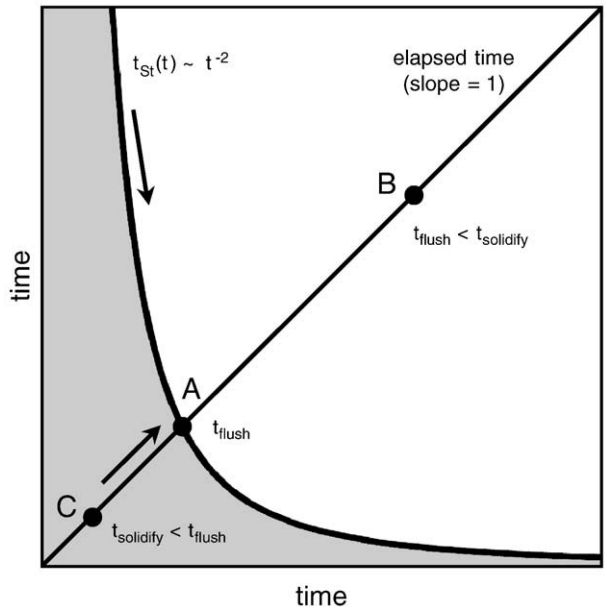

Fig. 3. Schematic illustrating the time dependence of the characteristic time of crystal settling, t_{St}, which decreases parabolically with time t. The elapsed time is represented by a line with slope 1. Crystals "flush" the sill when the crystal settling time decreases and matches the elapsed time (A). If the melt solidifies beforehand ($t_{solidify} < t_{flush}$), no crystal sedimentation will occur (C). A necessary criterion for crystal segregation is therefore $t_{flush} < t_{solidify}$, i.e. the solidification time has to be longer than the crystal settling time (B). This is the scenario we are concerned with in this work.

increases. Assuming spherical crystals, the crystal volume fraction Φ is given by

$$\Phi(t) = N(t)\frac{4}{3}\pi R(t)^3 \tag{3}$$

When the crystal volume fraction reaches a critical value, the melt–crystal mixture will experience a rheological transition and the remaining melt will be unable to flow around the crystals. At this point in time ($t_{solidify}$), the magma body solidifies in its current state. The critical crystal volume fraction is about 50–60% (e.g. McBirney and Murase, 1984) and in our model we use $\Phi_{solidify} = 50\%$. With the use of Eqs. (1)–(3) the time of solidification can be computed.

$$t_{solidify} = \left(\frac{3\Phi_{solidify}}{4\pi J G^3}\right)^{1/4} \tag{4}$$

In the absence of vigorous convection, crystals will sink through the melt with Stokes' velocity

$$v_{St}(t) = \frac{2\Delta\rho g R(t)^2}{9\eta} \tag{5}$$

where $\Delta\rho$ is the crystal/melt density difference, g is the acceleration due to gravity, and η is the melt viscosity. The characteristic time of crystal settling (t_{St}) is given by

$$t_{St}(t) = H/v_{St}(t) = \frac{9\eta H}{2\Delta\rho g G^2}\frac{1}{t^2} \tag{6}$$

where H is the vertical extent of the magma body. Since the crystal radius is a function of time, Stokes' velocity is a function of time and so is the characteristic time of crystal settling. This functional time dependence is shown in Fig. 3.

The characteristic time of crystal settling decreases as crystals grow. When the crystals are sufficiently large, their settling time decreases to the order of the time elapsed since the onset of nucleation and growth. These crystals sink to the bottom and drag along smaller crystals, effectively "flushing" the magma body. The time scale for this to occur (t_{flush}) is given by $t_{St}(t_{flush}) = t_{flush}$, which leads to

$$t_{flush} = \left(\frac{9H\eta}{2\Delta\rho g G^2}\right)^{1/3}. \tag{7}$$

In the proposed model, the formation of distinct layers occurs when crystals "flush" the crystal/melt mixture. "Flushing" must occur before the crystal volume fraction reaches the critical value at which it solidifies. A necessary condition for layer formation is therefore $t_{flush} < t_{solidify}$, which leads to a criteria for the melt viscosity η. Layer formation can only occur when the viscosity is lower than a critical viscosity η_{crit}, below which layer formation will occur.

$$\eta < \eta_{crit} \equiv \frac{2\Delta\rho g}{9H}\left(\frac{3\Phi_{solidify}}{4\pi J}\right)^{3/4} G^{-1/4}. \tag{8}$$

The thickness of the resulting layer can be estimated with a volumetric approach, using the volume fraction of crystals at the time when the system flushes.

$$h = \Phi(t_{flush})H = \frac{4\pi}{3}\left(\frac{9\eta}{2\Delta\rho g}\right)^{4/3} J G^{1/3} H^{7/3}. \tag{9}$$

The radius of the crystals that caused the flush-event can be predicted by

$$R_{cr} = R(t_{flush}) = \left(\frac{9HG\eta}{\Delta\rho g}\right)^{1/3}. \tag{10}$$

The effects of different variables on cumulate layer thickness h are shown in Fig. 4 for fixed magma body size, which we assume is generally known. It can be seen from Eq. (9) and Fig. 4a,b that layer thickness h correlates positively with viscosity ($\propto \eta^{4/3}$) because higher viscosities impose longer flush times, which in turn permits the accumulation of more suspended crystal mass prior to flushing. In line with our physical intuition, layer thickness also correlates with crystal nucleation rate ($\propto J$) and crystal growth rate ($\propto G^{1/3}$). There is also a dependence on magma chamber size ($\propto H^{7/3}$), but this quantity is generally considered to be known in the field.

Therefore, in order to extract paleo-viscosity out of cumulate layer thicknesses, constraints on crystal growth and nucleation rates are needed. Both of these quantities have been investigated in detail by Brandeis and Jaupart (1987). For the range of plausible magma conditions, they find ranges of 10^{-1} to 10^{3} m^{-3} s^{-1} and of 10^{-12} to 10^{-10} m/s for nucleation and growth rates, respectively. These ranges seem very large at first. However, if one knows the radii of crystals in the cumulate

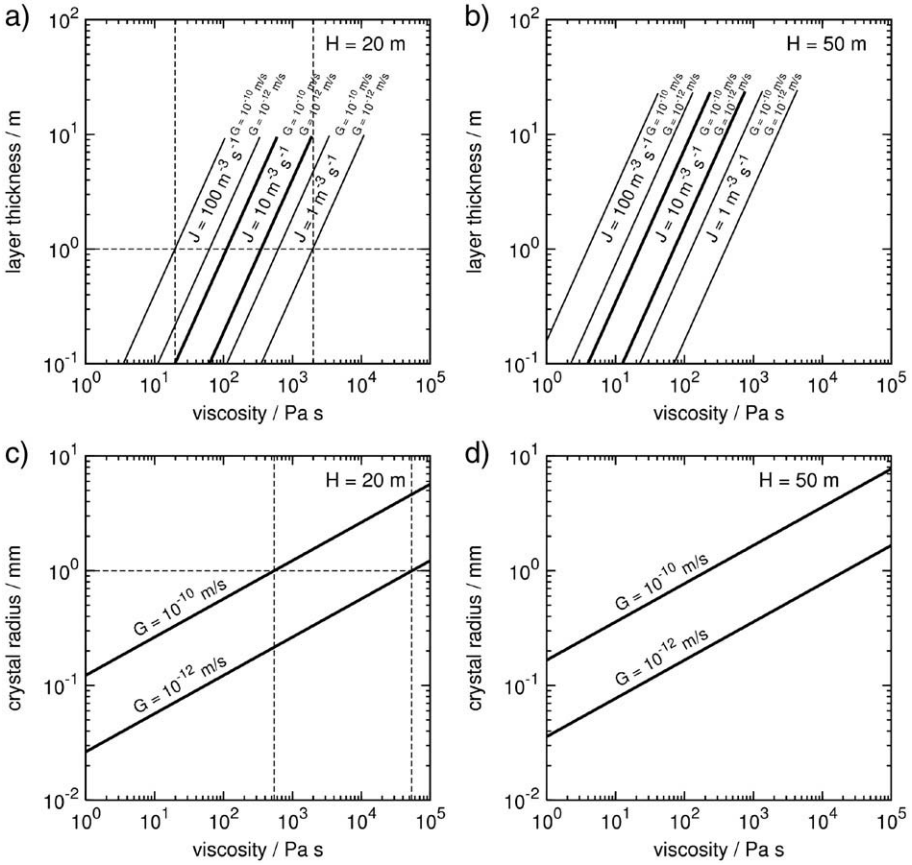

Fig. 4. Predicted layer thickness (a, b) and crystal size (c, d) as functions of viscosity for different magma chamber thicknesses H. Panels a, b: Each of the three bands represents a specific nucleation rate J, and their width reflects the range in the growth rate. The lines end at the critical viscosity as given by Eq. (8). Panels c, d: Width of the bands reflect range in growth rate. Estimates for J and G are taken from Brandeis and Jaupart (1987). Panels a and c also show how the viscosity can be constrained using layer thickness and grain size from field observations, which for the Big Bend example are shown as dashed horizontal lines. Given the range of nucleation and growth rates, one can read off minimum and maximum viscosities, which are indicated by dashed vertical lines. Using this method, the viscosity of the magma body can be obtained as the overlap of the two ranges given by the layer thickness criterion (a) and the crystal radius criterion (c). In the Big Bend example the magma viscosity can be constrained to $10^{2.7}$–$10^{3.3}$ Pa s.

layer, e.g., the critical radius at the flushing time, nucleation rates can be constrained to within 2 orders of magnitude. The uncertainties in growth rate are less of a concern because the dependence of cumulate layer thickness on growth rate scales only to the 1/3 power (Eq. (9)). Finally, because the critical crystal radius depends on the flush time (and vice versa), we can show that for a given growth rate the critical radius also correlates with viscosity (Eq. (10) and Fig. 4c,d).

5. Possible field applications

To illustrate how our analysis can potentially be applied in the field, we refer to the Big Bend outcrop that motivated our study. We state from the onset that our example here should be only taken as a preliminary case study, because we have not yet embarked on a detailed petrologic and structural investigation of this outcrop. In part, this is because the entire section is heterogeneously exposed and the rock is highly weathered. Thus, our study site may not be the perfect field site. Nevertheless, some of the rudimentary field observations presented here can be used to motivate dedicated field studies of better outcrops and application of the concepts outlined here.

We assume a density contrast of 500 kg/m^3 between crystals and melt, which is an average of hornblende, plagioclase and magnetite density contrasts with respect to a basaltic andesite. We show how the paleo-viscosity can be estimated using Fig. 4a, and c, which correspond to a 20 m thick magma chamber. Using a range of nucleation rates, J, and growth rates, G, (J=1 to 100 m^{-3} s^{-1}, G=10^{-12} to 10^{-10} m s^{-1}; see Brandeis and Jaupart (1987)), a layer thickness of 1 m yields instantaneous magma viscosities between $10^{1.3}$ and $10^{3.3}$ Pa s (Fig. 4a). An additional constraint on the viscosity is placed by the observed crystal radii (≈1 mm). From Fig. 4c one can read off the radii-constrained viscosity range as $10^{2.7}$ to $10^{4.7}$ Pa s. The viscosity range that satisfies both the cumulate layer thickness constraint and the crystal radius constraint is the overlapping viscosity range, which is $10^{2.7}$ to $10^{3.3}$ Pa s.

Our simple case study illustrates the potential usefulness of our model in extracting paleo-viscosity of a magma chamber. We caution that our model is only applicable to bodies which are large enough to retain heat (>1 m), but not so large (<1 km) that they undergo continued vigorous convection and re-entrainment of accumulated crystals. The model is therefore mostly applicable to sills or thick lava flows rather than large

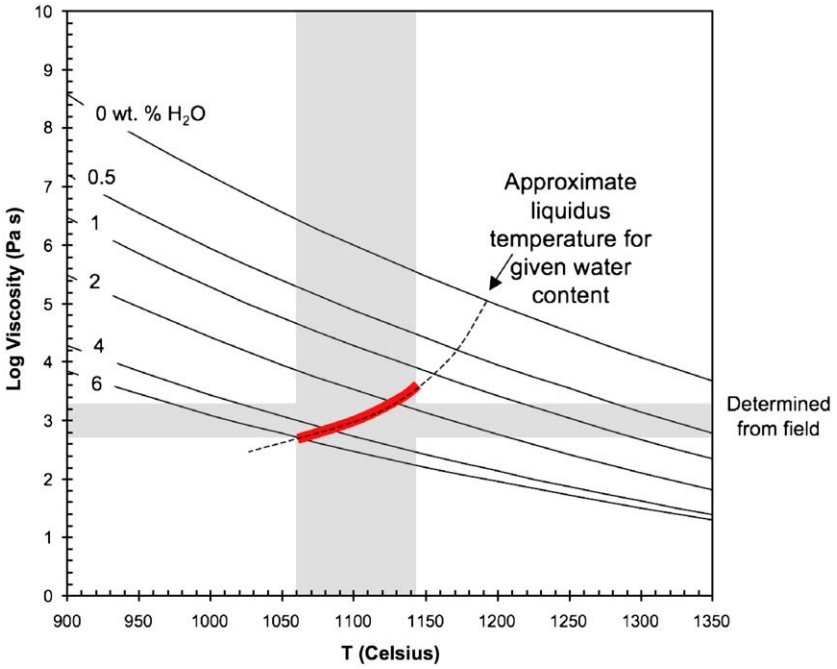

Fig. 5. Viscosity as a function of temperature, contoured against water content in terms of wt.%. Composition of magma is that of an evolved basalt given in the text. The viscosity parameterization is taken from Hui and Zhang (2007). Dashed line represents liquidus temperature of this magma for different water contents, calculated from the MELTS program (Ghiorso and Sack, 1995; Asimow and Ghiorso, 1998). Intersection of viscosity range with the liquidus curve (thick red line) gives an estimate of T and water content. Vertical grey bar denotes range of permissible T. Horizontal gray bar represents range of viscosities estimated from the thickness of the cumulate layers in Fig. 1 using our analysis in Fig. 4a and c. (For interpretation of the references to color in this figure legend, the reader is referred to the web version of this article.)

mafic intrusions, such as the Bushveld, Skaergaard, and Stillwater (Hess, 1960). The large mafic intrusions are characterized by very high Rayleigh numbers, which means that convective stresses need to be accounted for in any analysis of crystal settling in these large bodies (Sparks et al., 1993; Marsh, 1989). Despite these limitations, the analysis presented here provides the framework for a paleo-viscometer when combined with field observations of sills.

We now return to the implications for water content. As discussed in the Introduction, for a given composition, viscosity depends on temperature and water content to first order (Hui and Zhang, 2007; Dingwell, 1995). This is shown in Fig. 5 using the latest parameterizations of viscosity (Hui and Zhang, 2007) for a basaltic andesite composition (the anhydrous composition was assumed to be SiO_2=53.54, TiO_2=1.05, Al_2O_3=17.29, FeO=7.82, MnO=0, MgO=5.46, CaO=8.32, Na_2O=3.59, K_2O=1.64, P_2O_5=0.2 wt.%). We emphasize that this is just a rough composition estimate since we have not measured the composition of the parental magma of the cumulates. We have chosen it to simply show how our models could be applied. As Fig. 5 shows, if an independent constraint or bound on temperature can be estimated, the paleo-water content of the magma chamber can also be constrained. However, if the composition of the parental magma is roughly known, a slightly better constraint on both water content and temperature can be had. In Fig. 5 we plot the liquidus temperature of this magma as a function of water content as determined form the MELTS thermodynamic program (Ghiorso and Sack, 1995; Asimow and Ghiorso, 1998). Assuming that each cumulate layer is fractionally crystallized from the evolving magma liquidus of the magma, then the intersection of the viscosity with this curve provides an appropriate estimate of the water content and temperature of the magma that generated a given cumulate layer. For this study, the viscosity range translates into a water content of 3–6% and a temperature of 1050–1150 °C.

While this does not seem to be a very precise constraint on water content, it does allow us to conclude that the parental magma was wet. This inference is consistent with the presence of hornblende being observed as a primary liquidus phase in the cumulates. It is in ancient magmatic bodies where our inverse approach may prove most useful.

6. Conclusion

In conclusion, the analysis presented here provides a means of estimating viscosity of magma chambers from simple field relations. Viscosity in turn provides constraints on water content, which could have implications for settling some of the controversies over whether some ancient mafic magmas, such as komatiites, are wet or dry (Parman et al., 1997; Arndt et al., 1998) provided appropriate outcrops and independent temperature estimates exist. One approach for estimating magma temperatures is to use the MgO content of the magma, which correlates with temperature, but a potential problem is that water content can influence the relationship between MgO and temperature. However, recent studies have now parameterized the effect of water on Mg partitioning (Putirka, 2005), so it may be possible to back out temperature and water content by combining paleo-viscometry with thermobarometry.

Our analyses can also be applied to more evolved magmas. For example, with the advent of new thermometers, such as the

titanium in quartz thermometer (Wark and Watson, 2006), one could track how temperature, viscosity and water content evolve during progressive crystallization by mapping out stratigraphic variations in cumulate layer thickness and thermobarometric temperature. Collectively, such data could provide a new insight into magma dynamics.

Acknowledgments

The photograph in Fig. 1 was kindly provided by A. Agranier. We thank J. Morgan for discussions, and J.K. Russell and an anonymous reviewer for detailed and very helpful reviews. This research was supported by the NSF (Lee and Lenardic), the Packard Foundation (Lee) and Rice University's field trip endowment.

References

Arndt, N., Ginibre, C., Chauvel, C., Albarede, F., Cheadle, M., Herzberg, C., Jenner, G., Lahaye, Y., 1998. Were komatiites wet? Geology 26, 739–742.

Asimow, P.D., Ghiorso, M.S., 1998. Algorithmic modifications extending MELTS to calculate subsolidus phase relations. Am. Mineral. 83 (9–10), 1127–1132.

Brandeis, G., Jaupart, C., 1987. The kinetics of nucleation and crystal-growth and scaling laws for magmatic crystallization. Contrib. Mineral. Petrol. 96 (1), 24–34.

Burton, W.K., Cabrera, N., Frank, F.C., 1951. The growth of crystals and the equilibrium structure of their surfaces. Philos. Trans. R. Soc. Lond., A 243 (866), 299–358.

Campbell, I., 1996. Fluid dynamic processes in basaltic magma chambers. In: Cawthorn, R. (Ed.), Layered Intrusions. Elsevier, Amsterdam, Netherlands, pp. 45–76.

Dingwell, D., 1995. Viscosity and anelasticity of melts. In: Ahrens, T.J. (Ed.), Mineral Physics & Crystallography: A Handbook of Physical Constants. AGU Reference shelf, vol. 2. American Geophysical Union, pp. 209–217.

Ghiorso, M.S., Sack, R.O., 1995. Chemical mass transfer in magmatic processes IV. A revised and internally consistent thermodynamic model for the interpolation and extrapolation of liquid–solid equilibria in magmatic systems at elevated temperatures and pressures. Contrib. Mineral. Petrol. 119 (2), 197–212.

Gibb, F.G.F., Henderson, C.M.B., 1992. Convection and crystal settling in sills. Contrib. Mineral. Petrol. 109, 538–545.

Hess, H.H., 1960. Stillwater igneous complex, Montana: a quantitative mineralogical study. Geol. Soc. Am. 80.

Hort, M., Marsh, B.D., Spohn, T., 1993. Igneous layering through oscillatory nucleation and crystal settling in well-mixed magmas. Contrib. Mineral. Petrol. V114 (4), 425–440.

Hui, H., Zhang, Y., 2007. Toward a general viscosity equation for natural anhydrous and hydrous silicate melts. Geochim. Cosmochim. Acta 71, 403–416.

Kelley, K., Plank, T., Grove, T., Stolper, E., Newman, S., Hauri, E., 2006. Mantle melting as a function of water content beneath back-arc basins. J. Geophys. Res. 111 (B09208).

Koyaguchi, T., Hallworth, M.A., Huppert, H.E., Sparks, R.S.J., 1990. Sedimentation of particles from a convecting fluid. Nature 343, 447–450.

Koyaguchi, T., Hallworth, M.A., Huppert, H.E., 1993. An experimental study on the effects of phenocrysts on convection in magmas. J. Volcanol. Geotherm. Res. 55, 15–32.

Marsh, B.D., 1989. Magma chambers. Annu. Rev. Earth Planet. Sci. 17, 439–474.

Marsh, B.D., 2000. Magma chambers. In: Sigurdsson, H. (Ed.), Encyclopedia of Volcanoes. Academic Press, New York, pp. 191–206.

Martin, D., Nokes, R., 1988. Crystal settling in a vigorously convecting magma chamber. Nature 332, 534–536.

McBirney, A., Murase, T., 1984. Rheological properties of magmas. Ann. Rev. Earth Planet. Sci. 12, 337–357.

Naslund, H., McBirney, A., 1996. Mechanisms of formation of igneous layering. In: Cawthorn, R. (Ed.), Layered Intrusions. Elsevier, Amsterdam, Netherlands, pp. 1–43.

Nielsen, A., 1964. Kinetics of Precipitation. Pergamon, Tarrytown.

Ohara, M., Reid, R., 1973. Modeling crystal growth rates from solution. Prentice-Hall international series in the physical and chemical engineering sciences. Prentice-Hall, Englewood Cliffs, New Jersey.

Parman, S., Dann, J., Grove, T., de Wit, M., 1997. Emplacement conditions of komatiite magmas from the 3.49 Ga komati formation, Barberton Greenstone Belt, South Africa. Earth Planet. Sci. Lett. 150, 303–323.

Pons, J., Barbey, P., Nachit, H., Burg, J.P., 2006. Development of igneous layering during growth of pluton: The Tarcouate Laccolith (Morocco). Tectonophysics 413 (3–4), 271–286.

Putirka, K., 2005. Mantle potential temperatures at Hawaii, Iceland, and the mid-ocean ridge system, as inferred from olivine phenocrysts: evidence for thermally driven mantle plumes. Geochem. Geophys. Geosyst 6.

Rudman, M., 1992. Two-phase natural convection: implications for crystal settling in magma chambers. Phys. Earth Planet. Inter. 72, 153–172.

Solomatov, V.S., Stevenson, D.J., 1993. Suspension in convective layers and style of differentiation of a terrestrial magma ocean. J. Geophys. Res. 98, 5375–5390.

Sparks, R.S., Huppert, H.E., Koyaguchi, T., Hallworth, M.A., 1993. Origin of modal and rhythmic igneous layering by sedimentation in a convecting magma chamber. Nature 361, 246–249.

Spera, F.J., 2000. Physical properties of magma. In: Sigurdsson, H. (Ed.), Encyclopedia of Volcanoes. Academic Press, New York, pp. 171–190.

Sunagawa, I., 1984. Growth of crystals in nature. In: Sunagawa, I. (Ed.), Materials and Science of the Earth's Interior. Terra Scientific Publishing Company, pp. 63–105.

Tonks, W.B., Melosh, H.J., 1990. The physics of crystal settling and suspension in a turbulent magma ocean. In: Newsom, H.E., Jones, J.H. (Eds.), Origin of the Earth. Oxford Univ., New York, pp. 151–174.

Wark, D., Watson, E., 2006. TitaniQ: a titanium-in-quartz geothermometer. Contrib. Mineral. Petrol. 152, 743–754.

Zieg, M.J., Marsh, B.D., 2002. Crystal size distributions and scaling laws in the quantification of igneous textures. J. Petrol. 43 (1), 85–101.